

Paper Type: Original Article



Numerical Analysis of the Effect of Opposite Baffles on the Heat Transfer Enhancement of Non-Newtonian Nano Fluid through a Backward Facing Step

Kourosh Javaherdeh^{1,*} , Mehdi Moslemi², Motahareh Mahmoudnezhad³

¹Faculty of Mechanical Engineering, University of Guilan, Rasht, Iran; Javaherdeh@guilan.ac.ir.

²Department of Mechanical Engineering, Ayandegan Institute of Higher Education, Tonekabon, Iran; MehdiMoslemi1982@gmail.com.

³Department of Mechanical Engineering, Shahrood University of Technology, Shahrood, Iran; motahare.mahmoodnezhad@gmail.com.

Citation:



Javaherdeh, K., Moslemi, M., & Mahmoudnezhad, M. (2021). Numerical analysis of the effect of opposite baffles on the heat transfer enhancement of non-newtonian nano fluid through a backward facing step. *Big data and computing visions*, 1 (4), 216-231.

Received: 05/07/2021

Reviewed: 28/08/2021

Revised: 19/09/2021

Accept: 23/10/2021

Abstract

In this paper, the effect of opposite baffles on the flow field and the increase of forced heat transfer of non-Newtonian nanofluid flow in a laminar regime in a backward-facing step are investigated numerically. The finite volume method is used to solve the governing equations of flow and temperature. Besides, the impact of geometric parameters such as horizontal distance between baffles to the edge of the stairs and its numbers, like Reynolds number, nanoparticle volume fraction, and the non-Newtonian fluid behavior on the flow field and heat transfer have been examined. Results demonstrate that using non-Newtonian fluid instead of Newtonian fluid enhances heat transfer and reattachment length. Raising the Reynolds number and the nanofluid volume fraction causes the mean Nusselt numbers and the Performance Evaluation Index to increase. The outcomes indicate that using a pair of opposite baffles must be more beneficial than the other number of baffles.

Keywords: Backward facing step, Opposite baffles, Non-Newtonian nanofluid, Heat transfer enhancement, Numerical analysis.

1 | Introduction

Separation and reconnection of fluid flow occur due to sudden changes in canal geometry in many different industries, including transportation, air conditioning, aerospace, power plants, nuclear power, food, and petrochemicals. The stepped step model (BFS) is one of the most prevalent models for analyzing heat transfer and flow in sections using sudden expansion. This geometry has always been of interest to researchers because there is a return flow and an area in the corner of the back step where the minimum heat transfer rate occurs [1] and [2]. One of the adequate methods to improve heat transfer is to utilize efficient cooling fluid to raise heat performance in heat transfer systems. The use of non-Newtonian fluids in industrial applications has obtained extensive attention [3] and [4]. Moosavi et al. [3] numerically examined the heat transfer and flow pattern of viscoelastic



non-Newtonian fluid with a step back in a vertical channel. They revealed that the velocity and temperature boundary layer of viscoelastic non-Newtonian fluid is greater than a Newtonian fluid by comparing the outcomes of viscoelastic non-Newtonian fluid with Newtonian fluid. Furthermore, results demonstrated that the Nusselt number of viscoelastic non-Newtonian fluid is more elevated than that of a Newtonian fluid in the back step and in the flat plate. Danane et al. [4] studied the upsurge of Bingham fluid heat transfer within a back step channel and the influence of different backward step geometries on the fluid flow pattern numerically. They indicated the use of vertical stairs compared to curved and steep stairs raises the length of reconnection area of the flow and thus improves the pressure drop. Also, outcomes showed using sloping stairs increases the Nusselt number. Using baffles is another way to improve heat transfer inside the back step's duct [6], [7], [8]. Boruah et al. [5] analyzed raising heat transfer in a back step channel and the influence of different baffle geometries on the flow pattern. They indicated that utilizing rectangular baffles instead of elliptical and triangular baffles raises heat transfer and lessens the length of the reconnection area of the flow. The outcomes demonstrate the Nusselt number reaches its highest value around the baffle. They even observed that if the baffle position relative to the step grew, the pressure drops and the mean Nusselt number fell. Nie et al. [6] numerically analyzed the impact of the installation location of the baffle on fluid flow pattern and improved heat transfer within a back step channel. They discovered by changing the location of baffle installation, the location of the highest temperature and Nusselt number also changed. Furthermore, approaching the baffle position downstream enhances the heat transfer coefficient. Kumar and Vengadesan [7] numerically researched the upsurge of heat transfer in the laminar flow regime on a back step and the impact of baffle oscillation on the flow pattern. Outcomes illustrated that using oscillating baffles instead of fixed baffles makes a periodic flow and improves heat transfer. On the other hand, one of the inactive increasing heat transfer methods is adding nanoparticles to base fluid and creating nanofluids. Due to the inherent poor thermal conductivity in heat transfer of typical base fluids (such as water, ethylene glycol, and oils) adding solid nanoparticles impacts the base fluid's thermophysical properties such as viscosity, thermal conductivity, specific heat, and density and improves heat transfer [8]-[12] considerable investigations have been conducted to research the heat transfer and flow of nanofluids in the back step [8]-[12], which are mentioned below Pour and Nassab [8] numerically investigated the impact of different nanofluid types on their flow pattern and the growth of heat transfer in the laminar flow regime range in a back step. They indicated that by using nanofluids, heat transfer remarkably improved compared to the base fluid. Additionally, their results demonstrated that using aluminum and copper nanoparticles compared to other nanoparticles raises heat transfer. Togun et al. [9] analyzed nanofluids' heat transfer and the turbulent flow on a steep step numerically. They used water-based copper nanofluid and results indicated that the impact of utilizing nanofluids is growth by increasing the nanoparticles' volume fraction, Reynolds number, and heat transfer. Furthermore, increasing nanoparticles' volume fraction and Reynolds number, rises the pressure drop compared to the base fluid.

Chamkha and Selimefendigil [10] numerically analyzed the growth in heat transfer of nanofluid flow with oscillating inlet flow in a channel with a back step. They considered the impact of the oscillation frequency and amplitude of the oscillating current and the other shapes of the nanoparticles. Using spherical nanoparticles also improves the average Nusselt number by about 30.24%. Mohammed et al. [11] numerically examined the influence of rectangular, circular, and triangular barriers on the nanofluid flow's pattern and the heat transfer increase resulting from it in a backward step. Correspondingly, the ratio of mean Nusselt number to pressure drop called the performance evaluation index examined the growth in pressure drop and heat transfer simultaneously. They showed that in the triangular barrier, the mean Nusselt number and the performance of the appraisal index increase more than the other barriers. Nath and Krishnan [12] studied the heat transfer and mass transfer rates of the copper-water-based nanofluid's combined displacement within a back step, numerically. They investigated the influence of the ratio of buoyancy forces due to mass transfer to heat transfer, volume fraction, and Prandtl number of nanoparticles. Different values of buoyancy forces lead to the formation of various patterns in rotational currents close to the back step. Also, improving the volume fraction of nanoparticles raises the Nusselt number and the current's reconnection length.

Several limited investigations have been performed on the simultaneous usage of all three techniques of non-Newtonian fluids, inactivation of the baffle and nanofluids on the flow field, and enriching heat transfer within a stepped step [13]-[16]. Amiri et al. [13] investigated non-Newtonian nanofluid's heat transfer and turbulent flow on a back step, numerically. Their results indicated that the location of the maximum length and Nusselt number of reconnections is not related to the volume fraction of nanoparticles. Besides, the amount of Nusselt number and the maximum occurrence of Nusselt number increase with rising volume fraction and Reynolds number of nanoparticles. Heshmati et al. [14] numerically examined the influence of slotted baffle design on the improvement of heat transfer, nanofluid flow pattern, and pressure drop in a retrograde channel in the laminar flow range. They tested the performance of a system with four different nanoparticles (SiO_2 , Al_2O_3 , CuO , and ZnO), and their results showed that using SiO_2 nanoparticle improved the heat transfer compared to other ones. Slotted baffles even reduce pressure drop compared to conventional baffles. Their outcomes also showed that inclined baffles compared to the vertical baffles change the flow pattern and raise heat transfer. And using oblique and Nano fluid baffles raises the Nusselt number for Reynolds numbers 200 and 400 by 191% and 255%, respectively. Mohammed et al. [15] and [16] also examined the growth in nanofluid flow's heat transfer in a backward and a forward step and the effect of the geometric baffle configuration on the flow pattern numerically. They also investigated the impact of the nanoparticle volume fraction, Reynolds number, and the position of the baffle relative to the step, as well as the width and height of the baffle. Outcomes indicated that the installation position of the baffle comparative to the stairs has a significant impact on improving heat transfer. And the influence of baffle width on raising heat transfer is insignificant. Furthermore, they examined the influence of the baffle installation location on the bottom and top walls of the canal. The outcomes indicated that the heat transfer coefficient reaches its maximum value by installing a baffle on the upper wall of the duct.

Most previous examinations have analyzed the impact of parameters such as Reynolds number, type of Nano and non-Newtonian fluids, nanoparticles' volume fraction, heat transfer in the channel with a back step, and the baffle installation on the flow field. Issues such as the effect of non-Newtonian fluid behavior and the arrangement of reciprocating bundles on the thermal-hydraulic performance of the flow and the heat transfer of non-Newtonian Nano fluid within a stepped step have not yet been considered. Based on the examination of other researchers and regarding the lack of study of cross-bundle arrangement and the lack of performance evaluation index to analyze the flow pattern and heat transfer in different non-Newton Nano fluid flow conditions, the innovation of the present study is as follows. In this study, the forced displacement of non-Newtonian Nano fluids within a stepping step and the simultaneous evaluation of the effect of effective parameters on increasing heat transfer such as Reynolds number, nanoparticle volume fraction, and also the arrangement of cross bundles to change the flow pattern and its effect on heat transfer rate has been studied.

2 | Geometry of the Problem and Governing Equations

The schematic view of the two-dimensional geometry, the computational range of the problem, the installation location of the baffles, and the dimensions used are shown in *Fig. 1*. The stairs' height is $H = 1\text{cm}$, and the Expansion Ratio (ER), the ratio of the cross-sectional area after the stairs to the entrance cross-sectional area, is 2.

In *Table 1*, the non-Newton Nano fluid operating fluid with an aluminum oxide base fills the channel. Also, the thermodynamic properties of water, nanoparticles, and non-Newtonian Nano fluids with volume fractions of 0.5 and 1.5% are presented. This table also presents the properties of water-CMC solution for comparison pure water.

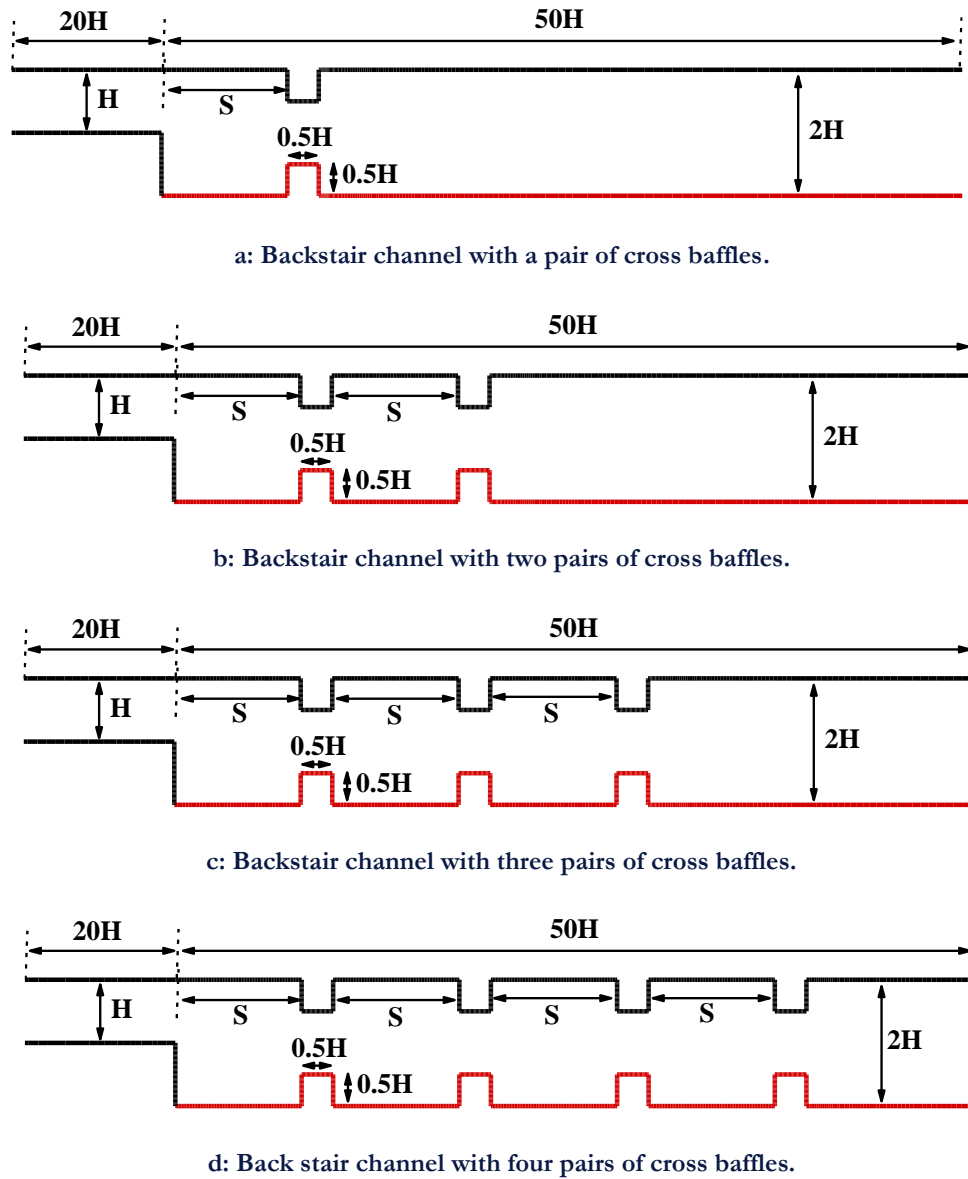


Fig. 1. Schematic view of the computational range for the number of different reciprocal baffles.

Table 1. Thermophysical properties.

Parameter	Water	Aluminum oxide	CMC (0.5%) + 0.5% Al_2O_3	CMC (0.5%) + 1.5% Al_2O_3
ρ	997.1	3970	1013.5	1040.5
K	0.613	40	0.6262	0.66
C_p	4179	765	4121	4012
Pr	6.2	-	-	-

Furthermore, in Table 2, the boundary conditions of temperature and velocity are summarized.

Table 2. Boundary conditions.

flow	Temperature	Border
$u = u_0, v = 0$	$T_{in} = 300 \text{ K}$	Channel input
$\partial u / \partial x = \partial v / \partial x = 0$	$\partial (T - T_m) / \partial x = 0$	Channel output
$u = v = 0$	$q'' = 0$	Top baffles
$u = v = 0$	$q'' = 3000 \text{ W/m}^2$	Bottoms' baffles
$u = v = 0$	$q'' = 3000 \text{ W/m}^2$	Heat flux wall down
$u = v = 0$	$q'' = 0$	Adiabatic walls

The equations governing the flow and transfer of heat, considering a continuous environment with a thermal balance between the base fluid and incompressible solid particles, are two-dimensional and laminar, including continuity, momentum, and energy conservation [4], [5] and [10]-[18].

Continuity:

$$\frac{\partial u}{\partial x} + \frac{\partial v}{\partial y} = 0. \quad (1)$$

Momentum:

$$u \frac{\partial u}{\partial x} + v \frac{\partial u}{\partial y} = -\frac{1}{\rho_{nf}} \frac{\partial P}{\partial x} + \frac{\mu_{nf}}{\rho_{nf}} \left(\frac{\partial^2 u}{\partial x^2} + \frac{\partial^2 u}{\partial y^2} \right). \quad (2)$$

$$u \frac{\partial v}{\partial x} + v \frac{\partial v}{\partial y} = -\frac{1}{\rho_{nf}} \frac{\partial P}{\partial y} + \frac{\mu_{nf}}{\rho_{nf}} \left(\frac{\partial^2 v}{\partial x^2} + \frac{\partial^2 v}{\partial y^2} \right). \quad (3)$$

Energy:

$$u \frac{\partial T}{\partial x} + v \frac{\partial T}{\partial y} = \frac{K_{nf}}{(\rho C_p)_{nf}} \left(\frac{\partial^2 T}{\partial x^2} + \frac{\partial^2 T}{\partial y^2} \right). \quad (4)$$

Water-CMC soluble exhibits plastic-like rheological behavior. Likewise, the apparent viscosity of this fluid can be obtained with the Power-law model as follows [17] and [18]:

$$\mu_A = B \dot{\gamma}^{(n-1)}. \quad (5)$$

In *Eq. (5)*, $\dot{\gamma}$, n and B represent the non-Newtonian fluid shear rate, Power law index, and stability, respectively. Based on the research of Hojjat et al. [17], N and B are calculated to evaluate the viscosity of non-Newtonian nanofluids.

To solve governing equations, it is necessary to define the thermodynamic properties of the nanofluid. Specific heat capacity and nanofluid density are determined based on the single-phase model as follows [10]-[14]:

$$\rho_{nf} = (1 - \phi) \rho_f + \phi \rho_p. \quad (6)$$

$$(\rho C_p)_{nf} = (1 - \phi) (\rho C_p)_f + \phi (\rho C_p)_p. \quad (7)$$

Eq. (8) shows the thermal conductivity of the nanofluid based on the Maxwell-Garnetts relation for spherical nanoparticles in the laminar flow regime range [18]:

$$K_{nf} = K_f \left[\frac{(K_f + 2K_p) - 2\phi(K_f - K_p)}{(K_f + 2K_p) + \phi(K_f - K_p)} \right]. \quad (8)$$

nf , f , P , and ϕ represent the nanofluid, the base fluid, the nanoparticles, and the volume fraction of nanoparticles, respectively.

The Reynolds number is also calculated according to the height of the stairs as follows:

$$Re = \frac{\rho_{nf} U_{in}^{2-n} H^n}{\mu_{nf}}. \quad (9)$$

In this equation, H is the step height, and U_{in} is the flow velocity at the input.

To evaluate the impact of cross-baffle installation and arrangement on non-Newton nanofluid flow and heat transfer, the local Nusselt number on the constant flux wall and the average Nusselt number according to Eq. (10) and (11) have been used:

$$Nu_x = \frac{h_x H}{K_{nf}} = \frac{H}{K_{nf}} \left(\frac{q''}{T_x - T_{in}} \right). \quad (10)$$

$$Nu_m = \frac{1}{50H} \int_0^{50H} Nu_x dx. \quad (11)$$

In Eq. (10), q'' is the constant heat flux transferred from the bottom wall surface to the fluid inside the back step channel, T_{in} is the inlet temperature of the flow and T_x is the local bottom wall temperature.

The pressure drop from Eq. (12) is also calculated:

$$\Delta P = P_{inlet} - P_{outlet}. \quad (12)$$

In relation (12), P_{outlet} and P_{inlet} are the average pressure at the outlet and inlet sections, respectively.

Besides, the performance evaluation index is calculated according to Eq. (13) to simultaneously estimate the growth in heat transfer and pressure drop due to the presence of the baffle [8]:

$$\eta = \frac{(Nu_m/Nu_{m0})}{(\Delta P_m/\Delta P_{m0})^{(1/3)}}. \quad (13)$$

In this equation, Nu_m and ΔP_m are the average Nusselt number and the flow pressure drop in the channel with the back step in the presence of reciprocating bundles, respectively. Also, Nu_{m0} and ΔP_{m0} are the average Nusselt number and the flow pressure drop in the channel with back step without baffle, respectively.

3 | Numerical Simulation

In this study, Ansys-Fluent 18 software was used to solve the governing equations numerically. The governing equations are discretized based on the finite volume technique. The fluid flow equations are implicitly simulated in the steady-state by the pressure-based solvent.

To discretize the pressure and other terms of the equation, the standard method and the second-order approximation, the terms containing the gradient by the least-squares gradient method, respectively, have been used. The SIMPLE algorithm is used to solve the pressure and velocity fields simultaneously. To detect convergence, the reduction criterion of the balanced residues is 10^{-8} . Furthermore, monitoring the changes of substantial flow quantities in sensitive areas is considered a convergence criterion. In the simulations of this study, the subtraction coefficients are adjusted to achieve better convergence to solve the equations. Values of under relaxation factor for the momentum, pressure, and energy equations were selected to be 0.6, 0.3, and 0.6, respectively. Gambit 2.4 commercial software has been used to grid the computing area in an organized, rectangular and non-uniform manner. Higher grids have been used to raise the accurateness of calculations in places close to walls, fines and folds that have a strong gradient. In

addition, the computing area is separated into various areas to control the production network better. *Fig. 2* illustrates a sight of the computational network around the channel layers.

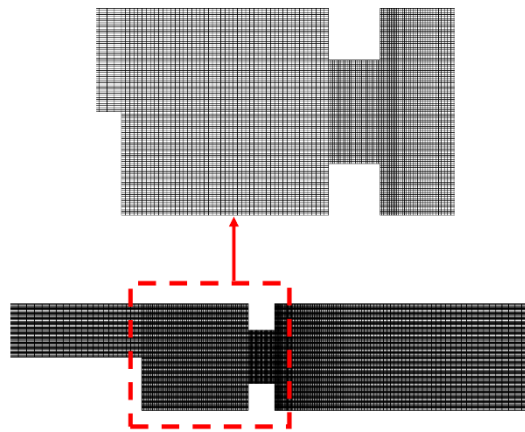


Fig. 2. Computing space networking.

The mean Nusselt number on the hot wall of the back step channel was selected as the grid independence parameter to analyze the independence of the numerical solution outcomes from the computational grid. As can be seen in *Table 3*, for geometry with a pair of reciprocating baffles, four different lattices in a volume fraction of 0.015 and the Reynolds number 200 have been used. As shown in *Table 3*, changing the number of grids from 61910 to 83424 causes a slight difference in the answers, so the network with 61910 has better computational accuracy and time and is selected as the appropriate network. The independence of numerical solutions from the network for other conditions has also been examined.

Table 3. Grid independence for the arrangement of a pair of cross baffles for non-Newton nanofluids at a volume fraction of 1.5% and Reynolds number 200 at $S = H$.

Grid	Number of cells	Mean Nusselt Number
Grid 1	15488	14.12
Grid 2	35620	13.58
Grid 3	61910	13.72
Grid 4	83424	13.71

3.1 | Validation

The distribution of Nusselt number on the hot wall of a smooth channel is compared with the results of Akbari et al. [19] for non-Newtonian nanofluids for Reynolds numbers 500 and 1000 in *Fig. 3*. On the other hand, the length of their calculation area is $100H$, of which $30H$ is the initial length of the walls with the thermal insulation boundary condition. The numerical results of the present study and their experimental results correspond to acceptable accuracy. Furthermore, to evaluate the accuracy of the numerical outcomes of fluid flow, the velocity distribution per Reynolds number 100, at different stages after the step, is compared with the experimental results of Armaly et al. [20] for the fluid flow of water inside the back step in *Fig. 4*. The length of the calculation area of this geometry from the entrance of the channel to the edge of the stairs and from the edge of the stairs to the exit of the channel is 20 and 50 cm, respectively. The height of the channel and the ER are 1.01 cm and 1.94, respectively. In this case, too, the numerical results and the experimental results are close to each other.

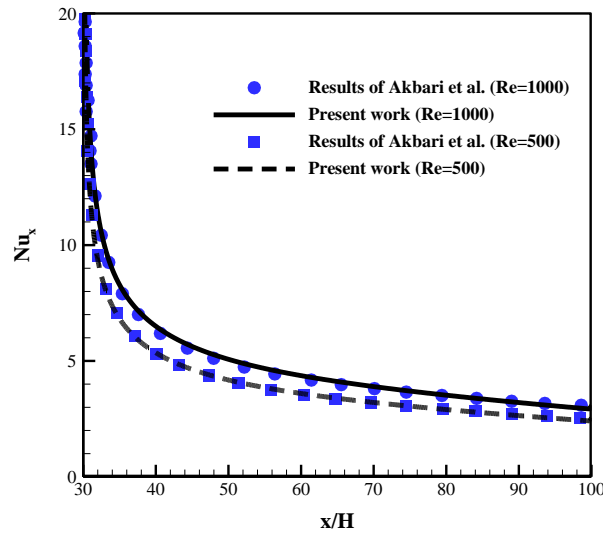


Fig. 3. Comparison of Nusselt number distribution of non-Newton nanofluid on the hot wall of a smooth channel for different Reynolds numbers.

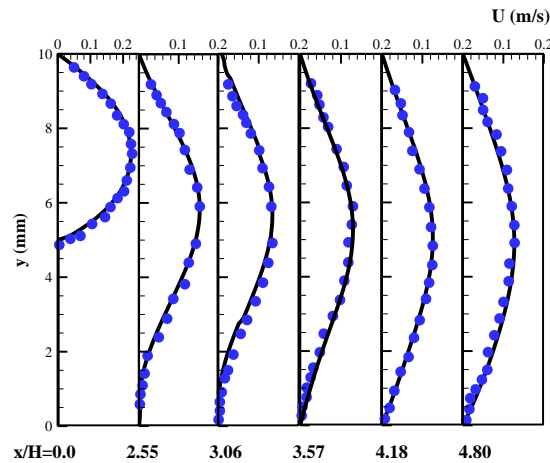


Fig. 4. Comparison of velocity distribution with the experimental results of Armaly et al. [23] for $Re = 100$ at different x / H sections).

4 | Results and Discussion

In this research, the impact of different baffle arrangements within a channel with a back step in the presence of non-Newtonian nanofluid has been examined. The influence of parameters such as Reynolds number and volume fraction of nanoparticles, number of bundles, and horizontal distance of bundles to the edge of the step has also been evaluated. To evaluate the impact of these parameters, results are presented in the form of temperature distribution, flow lines, mean Nusselt number as well as the performance evaluation index. In this section, first, the behavior of non-Newtonian fluid (water + 0.5% CMC) with pure water fluid is compared. Fig. 5 illustrates the effect of using non-Newtonian fluid instead of water in the Reynolds 200 for back-channel flow lines. The results indicate that the use of non-Newtonian fluid causes a significant change in the flow pattern and vortex after the step. Besides, the reconnection length for non-Newtonian fluid is diminished compared to Newtonian fluid. And the size of the vortex formed after the stairs was also reduced by using non-Newtonian fluid.

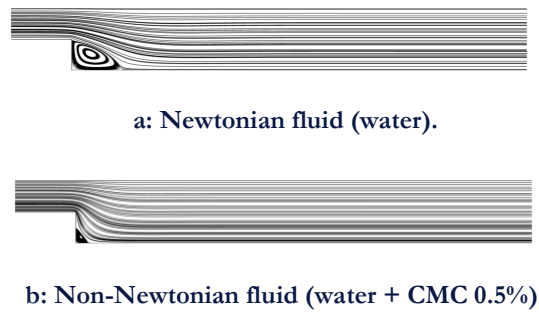


Fig. 5. Flow lines around the back step in Reynolds number 200.

Also, in *Fig. 6*, to evaluate the behavior of non-Newtonian fluid (water + 0.5% CMC) on improving heat transfer, the distribution of local Nusselt number on a fixed flux wall for a channel with a back step in Reynolds number 200 is shown. As can be seen, the Nusselt number of the non-Newtonian fluid is higher than that of the Newtonian fluid (water), which indicates the advantage of using non-Newtonian fluids to improve heat transfer. Investigating the effect of arrangement and number of reciprocating bundles on the flow pattern, flow lines for different arrays of reciprocating baffles in Reynolds number 200, and volume fraction of 0.015 nanoparticles are shown in *Fig. 7*. By the presence of baffles in the canal with a back step, the flow pattern changes, especially around the baffles. And as the number of baffles changes, so does the number and size of vortices form around the baffles. Also, by changing the number of baffles, the size of the initial vortex after the step remains almost the same. The results indicate that the presence of baffles in the channel with the back step causes the flow to be diverted and the boundary layer to be disturbed, which improves the heat transfer compared to the channel without the baffle.

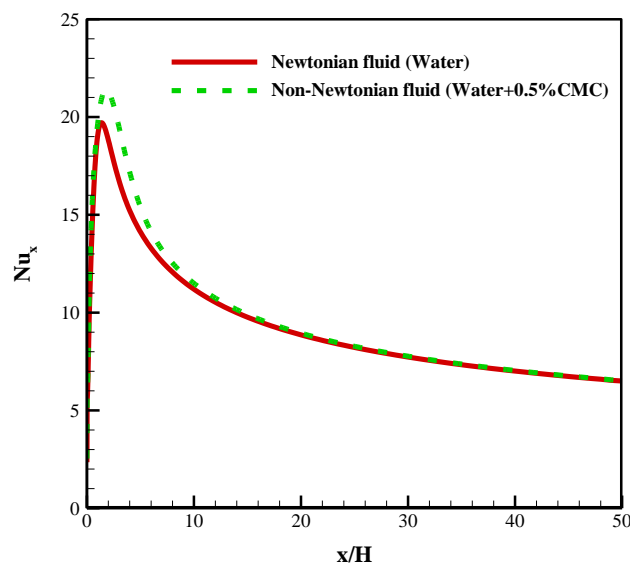
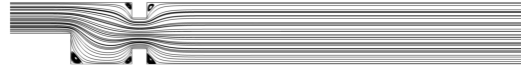


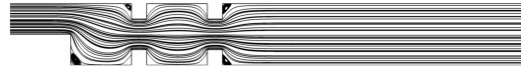
Fig. 6. Distribution of Nusselt number on the fixed flux wall of the back step channel in Reynolds number 200.



a: Back stairs without baffle.



b: Back stairs with a pair of baffles.



c: Back stairs with two pairs of baffles.



d: Back stairs with three pairs of baffles.



e: Back stairs with four pairs of baffles.

Fig. 7. Flow lines around the back steps and baffles ($\varphi=0.015$, $S=2H$, $Re=200$).

Furthermore, to evaluate the effect of the number of reciprocating baffles on the thermal characteristics inside the back step channel, the temperature distribution according to the number of baffles in Reynolds number 200 for non-Newton nanofluid flow with a volume fraction of 0.015 nanoparticles is illustrated in Fig. 8. By changing the number of baffles, there is a significant change in the temperature distribution within the channel with the back step. And the temperature in the corners of the baffles has a maximum value due to the presence of small vortices trapped in this area. The outcomes show that by raising the number of reciprocating baffles, the maximum temperature rises. In addition, the presence of reciprocating baffles and a difference in their number cause a significant change in the temperature distribution near the hot wall as well as the turbulence of the thermal boundary layer.

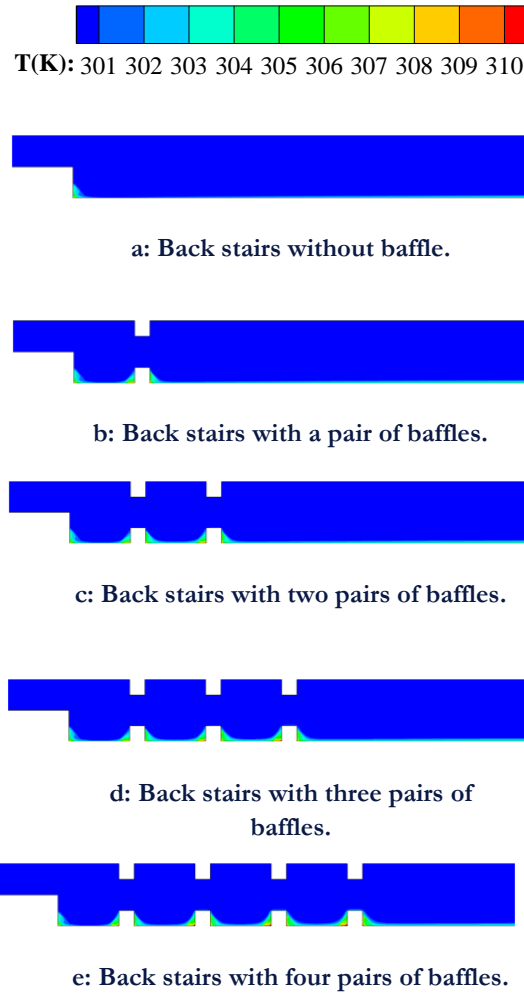


Fig. 8. Temperature distribution around back steps and baffles ($\varphi=0.015$, $S=2H$, $Re=200$).

The longitudinal distribution of the Nusselt number on a constant flux wall to evaluate the heat transfer in different arrangements of the number of reciprocating baffles is shown in Fig. 9. As the number of baffles grows, so does the number of peaks in the Nusselt number diagram. As the number of baffles increases, the vaster area of the back step channel, especially around the baffles, has a lower cross-section and more velocity, which increases the heat transfer term compared to the conduction heat transfer term, thus raising the Nusselt number. As it moves away from this region and approaches the output, the non-Newton nanofluid stream reaches development, and the Nusselt number of developments is the same in all cases.

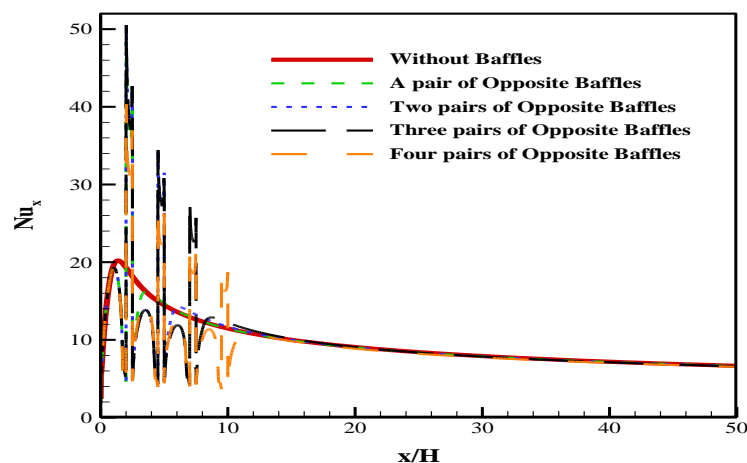
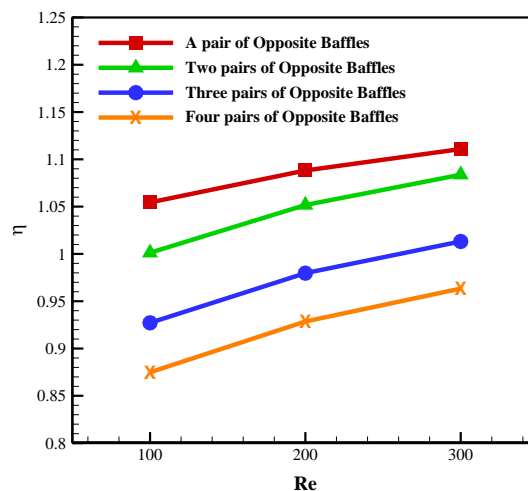


Fig. 9. Distribution of Nusselt number on a constant flux wall according to the number of different reciprocating baffles ($\varphi=0.015$, $S=2H$, $Re=200$).

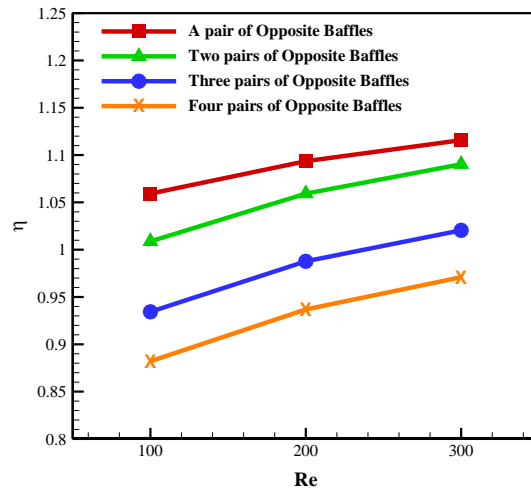
Considering that the number of reciprocating baffles is one of the design parameters inside the channel with a back step and the parameter affecting the flow and heat transfer, it is necessary to study its influence on improving heat transfer.

Fig. 10 illustrates the ratio of "average Nusselt number with cross baffles" to "average Nusselt number without cross baffles" in terms of several baffles for Reynolds numbers and different volume fractions for different values of horizontal baffles distance from the edge of the stairs. This ratio is an acceptable measure of the increase in heat transfer.

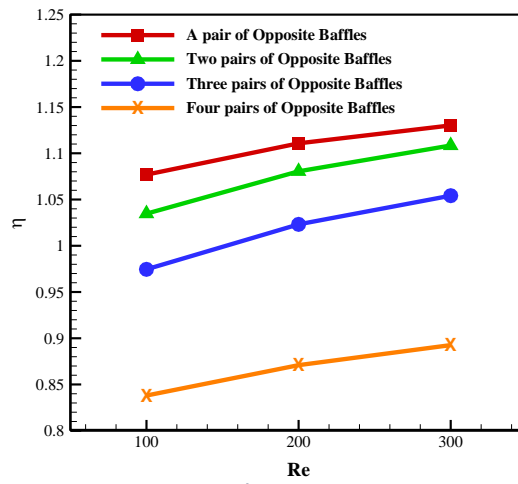
In all cases, the growth in the average Nusselt number for the arrangement of a pair of reciprocal baffles has a maximum value compared to the other number of baffles. Also, with increasing Reynolds number in the range of 100 to 300, the average Nusselt number has increased. As the volume fraction of nanoparticles to the base fluid increases, the thermal conductivity of the fluid increases, so the average Nusselt number ratio grows with the volume fraction of the nanoparticles. So that the maximum value of Num / Num_0 for Reynolds number 300 and $S = 2H$ in volume fraction of 0.005 and 0.015 are about 1.143 and 1.148, respectively. As the number of reciprocal baffles increases to two pairs, the Nusselt number ratio increases, and with further gain in the number of baffles to three and four, the Nusselt number ratio declines, and in some cases even falls below one. In addition, the horizontal distance of the baffles is also one of the parameters affecting the results. The outcomes indicate that for $S=2H$, the Nusselt number ratio will improve more to other conditions. On the other hand, due to the change in the flow pattern and the size of the vortices around the reciprocating baffles, by changing the number of baffles, the pressure drop also changes. To simultaneously evaluate the increase in heat transfer and pressure drop due to changes in the number of baffles, the performance evaluation index (η) in terms of the number of baffles for Reynolds numbers and different volume fractions for different values of the horizontal distance of the baffles to the edge of the step is shown in Fig. 11. As displayed in this figure, the maximum values of the performance appraisal index occur in the arrangement of a pair of cross baffles. Furthermore, the performance evaluation index in all conditions for the arrangement with a pair of reciprocating baffles has a value greater than 1, which indicates the effectiveness of the presence of baffles on thermal efficiency. On the other hand, raising the Reynolds number and volume fraction of nanoparticles improves the performance evaluation index. The results also demonstrate that for $S=2H$, the performance evaluation index is higher than other conditions. According to this figure, the maximum values of performance evaluation index per Reynolds number 300 and $S=2H$ in volume fraction of 0.005 and 0.015 are about 1.130 and 1.134, respectively, which indicates the effectiveness of reciprocating baffles on efficiency. It is the heat for the flow of non-Newtonian nanofluid into a channel with a back step.



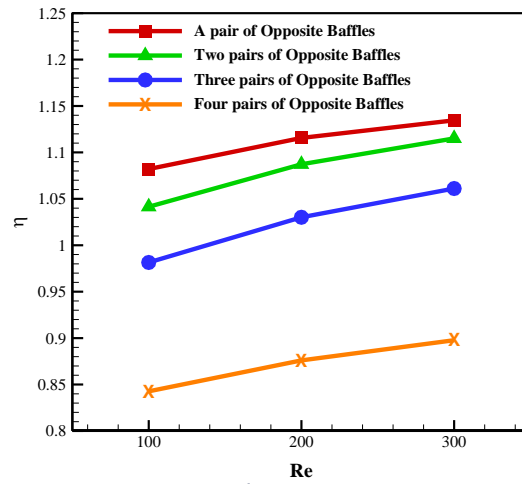
a: $\varphi=0/005$, $S=H$.



b: $\phi=0/015$, $S=H$.



c: $\phi=0/005$, $S=2H$.



d: $\phi=0/015$, $S=2H$.

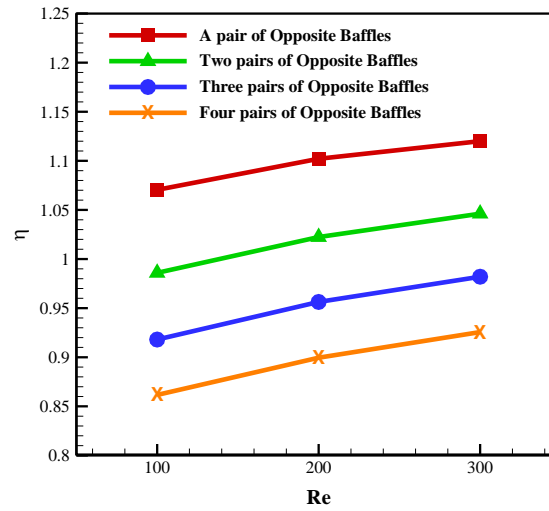
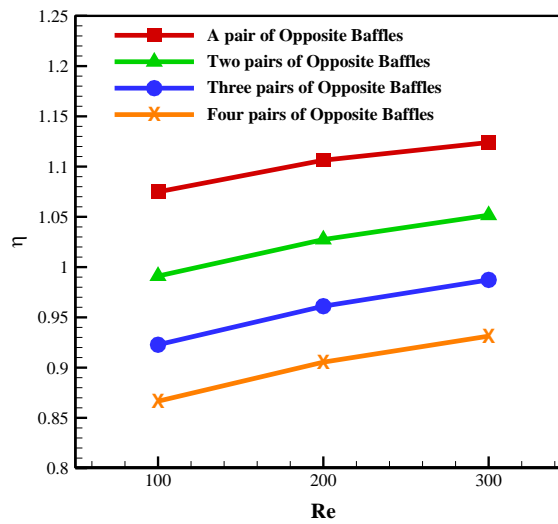

e: $\varphi=0/005$, $S=3H$.

f: $\varphi=0/015$, $S=3H$.

Fig. 11. Performance evaluation index in terms of number of baffles for Reynolds numbers and different volume fractions for different values of horizontal distance of baffles to the edge of the stairs.

5 | Conclusion

In this study, the effect of cross-baffles presence on the flow pattern and the increase in heat transfer of forced displacement of non-Newtonian copper nanofluid with water base + 0.5% CMC in the laminar regime range on a back step has been numerically studied. The main purpose of this investigation is to simultaneously evaluate the effect of geometric parameters such as horizontal distance between baffles to the edge of the stairs and its number as well as Reynolds number, nanoparticle volume fraction, and non-Newtonian fluid behavior on flow pattern and heat transfer. A performance evaluation index is also defined to simultaneously evaluate the increase in heat transfer and pressure drop. The results demonstrate that using non-Newtonian fluid in comparison with Newtonian fluid increases the maximum amount of Nusselt number and decreases the length of reconnection in the flow inside the channel with the back step. The outcomes reveal that with increasing Reynolds number and volume fraction of nanoparticles, the average Nusselt number and performance evaluation index increase in a certain arrangement. In addition, the presence of reciprocal baffles in the canal with the back step raises the number of local Nusselt, especially near the baffles. The results also indicate that increasing the number of baffles does not necessarily improve the performance evaluation index and heat transfer, so that for a pair of reciprocating baffles, the average Nusselt number and the performance evaluation index have the maximum value in all conditions.

The authors declare that they have no conflicts of interest.

References

- [1] Qi, C., Ding, Z., Tu, J., Wang, Y., & Wang, Y. (2021). Study on backward-facing step flow and heat transfer characteristics of hybrid nanofluids. *Journal of thermal analysis and calorimetry*, 144(6), 2269-2284. <https://doi.org/10.1007/s10973-020-10379-6>
- [2] Nath, R., & Murugesan, K. (2021). Numerical investigation of double-diffusive mixed convection of Fe₃O₄/Cu/Al₂O₃-water nanofluid flow through a backward-facing-step channel subjected to magnetic field. *International journal of numerical methods for heat & fluid flow*, 32(3), 889-914. <https://doi.org/10.1108/HFF-02-2021-0151>
- [3] Moosavi, R., Moltafet, R., & Shekari, Y. (2021). Analysis of viscoelastic non-Newtonian fluid over a vertical forward-facing step using the Maxwell fractional model. *Applied mathematics and computation*, 401, 126119. <https://doi.org/10.1016/j.amc.2021.126119>
- [4] Danane, F., Boudiaf, A., Mahfoud, O., Ouyahia, S. E., Labsi, N., & Benkahla, Y. K. (2020). Effect of backward facing step shape on 3D mixed convection of Bingham fluid. *International journal of thermal sciences*, 147, 106116. <https://doi.org/10.1016/j.ijthermalsci.2019.106116>
- [5] Boruah, M. P., Randive, P. R., & Pati, S. (2018). Hydrothermal performance and entropy generation analysis for mixed convective flows over a backward facing step channel with baffle. *International journal of heat and mass transfer*, 125, 525-542. <https://doi.org/10.1016/j.ijheatmasstransfer.2018.04.094>
- [6] Nie, J., Chen, Y., Boehm, R. F., & Hsieh, H. T. (2007, January). Parametric study of turbulent separated convection flow over a backward-facing step in a duct. In *Fluids engineering division summer meeting* (Vol. 42886, pp. 997-1004). <https://doi.org/10.1115/FEDSM2007-37315>
- [7] Kumar, S., & Vengadesan, S. (2019). The effect of fin oscillation in heat transfer enhancement in separated flow over a backward facing step. *International journal of heat and mass transfer*, 128, 954-963. <https://doi.org/10.1016/j.ijheatmasstransfer.2018.09.001>
- [8] Pour, M. S., & Nassab, S. G. (2012). Numerical investigation of forced laminar convection flow of nanofluids over a backward facing step under bleeding condition. *Journal of mechanics*, 28(2), N7-N12. DOI: <https://doi.org/10.1017/jmech.2012.45>
- [9] Togun, H., Safaei, M. R., Sadri, R., Kazi, S. N., Badarudin, A., Hooman, K., & Sadeghinezhad, E. (2014). Numerical simulation of laminar to turbulent nanofluid flow and heat transfer over a backward-facing step. *Applied mathematics and computation*, 239, 153-170. <https://doi.org/10.1016/j.amc.2014.04.051>
- [10] Chamkha, A. J., & Selimefendigil, F. (2018). Forced convection of pulsating nanofluid flow over a backward facing step with various particle shapes. *Energies*, 11(11), 3068. <https://doi.org/10.3390/en11113068>
- [11] Mohammed, H. A., Fathinia, F., Vuthaluru, H. B., & Liu, S. (2019). CFD based investigations on the effects of blockage shapes on transient mixed convective nanofluid flow over a backward facing step. *Powder technology*, 346, 441-451. <https://doi.org/10.1016/j.powtec.2019.02.002>
- [12] Nath, R., & Krishnan, M. (2019). Numerical study of double diffusive mixed convection in a backward facing step channel filled with Cu-water nanofluid. *International journal of mechanical sciences*, 153, 48-63. <https://doi.org/10.1016/j.ijmecsci.2019.01.035>
- [13] Amiri, A., Arzani, H. K., Kazi, S. N., Chew, B. T., & Badarudin, A. (2016). Backward-facing step heat transfer of the turbulent regime for functionalized graphene nanoplatelets based water-ethylene glycol nanofluids. *International journal of heat and mass transfer*, 97, 538-546. <https://doi.org/10.1016/j.ijheatmasstransfer.2016.02.042>
- [14] Heshmati, A., Mohammed, H. A., & Darus, A. N. (2014). Mixed convection heat transfer of nanofluids over backward facing step having a slotted baffle. *Applied mathematics and computation*, 240, 368-386. <https://doi.org/10.1016/j.amc.2014.04.058>
- [15] Mohammed, H. A., Alawi, O. A., & Wahid, M. A. (2015). Mixed convective nanofluid flow in a channel having backward-facing step with a baffle. *Powder technology*, 275, 329-343. <https://doi.org/10.1016/j.powtec.2014.09.046>
- [16] Mohammed, H., Alawi, O. A., & Sidik, N. C. (2016). Mixed convective nanofluids flow in a channel having forward-facing step with baffle. *Journal of advanced research in applied mechanics*, 24(1), 1-21.

- [17]Hojjat, M., Etemad, S. G., & Bagheri, R. (2010). Laminar heat transfer of non-Newtonian nanofluids in a circular tube. *Korean journal of chemical engineering*, 27(5), 1391-1396. <https://doi.org/10.1007/s11814-010-0250-3>
- [18] Abu-Nada, E. (2008). Application of nanofluids for heat transfer enhancement of separated flows encountered in a backward facing step. *International journal of heat and fluid flow*, 29(1), 242-249. <https://doi.org/10.1016/j.ijheatfluidflow.2007.07.001>
- [19] Akbari, O. A., Toghraie, D., Karimipour, A., Marzban, A., & Ahmadi, G. R. (2017). The effect of velocity and dimension of solid nanoparticles on heat transfer in non-Newtonian nanofluid. *Physica E: low-dimensional systems and nanostructures*, 86, 68-75. <https://doi.org/10.1016/j.physe.2016.10.013>
- [20] Armaly, B. F., Durst, F., Pereira, J. C. F., & Schönung, B. (1983). Experimental and theoretical investigation of backward-facing step flow. *Journal of fluid mechanics*, 127, 473-496. DOI: <https://doi.org/10.1017/S0022112083002839>